Journal of Electroceramics, 13, 223–227, 2004

Nonlinear Microwave Properties of Ferroelectric Thin Films

R. WÖRDENWEBER, R. OTT & P. LAHL
ISG2, CNI, Forschungszentrum Jülich, 52425 Jülich, Germany

Submitted February 13, 2003; Revised July 29, 2003; Accepted January 30, 2004

Abstract. The nonlinear microwave properties of ferroelectric $SrTiO_3$ thin films are characterized via complex analysis of the intermodulation distortion (IMD) signals up to high microwave power. The measurements reveal an unusual dependence of the IMD signals on the input power, which indicates the presence of two different nonlinear properties being responsible for the generation of the intermodulation. IMD measurements on tuned ferroelectric films and simultaneous conductivity measurements reveal the two different properties to be the nonlinear permittivity at low rf power and a finite nonlinear conductivity at high rf power levels, respectively. The IMD signal strength can not be explained in terms of the classical description based on a Taylor expansion of the nonlinear parameter. In contrast, simulations of the frequency spectra using more appropriate descriptions of two nonlinear parameters yield an excellent agreement between theory and experiment, and, thus, demonstrate, that the IMD experiments together with the simulation might provide further insight into the mechanism of nonlinear behavior of these material.

Keywords: ferroelectrics, thin films, nonlinear microwave properties, inter modulation distortion

Introduction

The rapid development of microwave applications in a broad variety of technologies (e.g. communication, radar, anticollision systems etc.) has triggered a strong demand for frequency-tunable resonators and filters operating in the GHz regime. Thin films of ferroelectrics such as $BaTiO_3$ and $SrTiO_3$ (STO) provide high relative permittivity ε which can be modified by a dc electric field, i.e., $\varepsilon = \varepsilon(E)$. Therefore, these materials can be utilized in tunable capacitors for electronic devices. In contrast to bulk dielectrics, they can be integrated into small complex thin-film devices and, for instance, be used in combination with perovskite superconductors of extremely low rf losses. However, up to the present a few problems inherent to these materials have to be solved. These are mainly (i) the relatively high dielectric losses, (ii) the large temperature dependence $d\varepsilon/dT$ in the temperature range of tuneability and (iii) the nonlinear behavior of ε at high levels of microwave power. The latter effect has not attracted too much interest up to now. However, in case of device integration and miniaturization, the tunable elements can be exposed to large rf-power. Thus, nonlinear effects will become important and might lead to changes in the device performance, higher harmonics and intermodulation distortion (IMD).

In this paper we will focus on the nonlinear dielectric properties of ferroelectric thin films. The nonlinear dielectric properties are analyzed by measurements of 3rd (and higher) order IMD signals on STO thin film varactors. The experimental results are compared with theoretical predictions in terms of Taylor expansions of the nonlinear relative permittivity $\varepsilon(E)$ and numerical simulations. It is shown, that the usual description (Taylor expansion) can not explain the experiments properly. In contrast, the numerical simulations using two sets of parameters for the nonlinearity reveal an excellent agreement and demonstrate, that the IMD experiments together with the simulation might provide further insight into the mechanism of nonlinear behavior of these materials.

Experimental Results and Discussion

Due to the small microwave losses and the compatibility with ceramic superconductors, CeO_2-buffered r-cut

sapphire (Al_2O_3) is used for the deposition of STO films. The films are grown via on-axis magnetron rf sputtering technique in a gas mixture of Ar and O_2. Typical deposition parameters are: 130 and 260 W rf power, 13 Pa and 3.5–10 Pa (optimum at 3.5 Pa), 830°C and 650–870°C heater temperature for CeO_2 and STO, respectively. Whereas CeO_2 grows completely (200)-oriented with a full width at half maximum (FWHM) of $\Delta\omega \approx 0.8$–1.3°, two different epitaxial structural orientations are observed in the STO layers. The structural orientation of STO strongly depends on gas pressure and substrate temperature during deposition. At low process pressure and temperature, STO growths predominantly (110) oriented, at higher temperature $T_H > 840^\circ$C the (111)-oriented phase starts to take over. In contrast to STO films on $LaAlO_3$ or sapphire without buffer, (100)-oriented STO can not be detected in these films.

The dielectric properties are determined by capacity measurements at 1 KHz, 1 MHz, and 2 GHz on planar capacitors consisting of STO films covered with Au electrodes forming capacitor gaps ranging from 2 to 10 μm. The relative permittivity is typically $\varepsilon(300\ \mathrm{K}) \approx 120$–$600$ with a maximum of $\varepsilon(55$–$65\ \mathrm{K}) \approx 150$–$800$, which is comparable to literature data [1, 2]. The dielectric losses are very low, i.e. $\tan\delta(300\ \mathrm{K}) \approx 0.002$–$0.005$ with a maximum of $\tan\delta(35$–$55\ \mathrm{K}) \approx 0.005$–$0.015$. They are small compared to typical literature data for STO films on sapphire [3] and comparable to the best values obtained via post-annealing treatment of STO on $LaAlO_3$ [4]. The Curie point of about 50–60 K for our films is slightly smaller than the value of ~90 K reported for sputtered STO films in the literature [5]. The capacity tuneability $n = C(0\ \mathrm{V})/C(U_{dc})$ scales with ε and ranges from $n = 1.2$ to 2.0 for $U_{dc} = 100$ V (see Fig. 1). All dielectric properties are strongly influenced by the strain of the STO film that is induced by the lattice mismatch between substrate and STO. As an example, Fig. 1 shows a plot of the correlation between the dielectric constant ε and the lattice mismatch. The data can nicely be explained in terms of the thermodynamic Landau theory based on the minimization of the free energy of a distorted cubic ferroelectric material [6, 7]. An extensive discussion of the structural properties and their impact on the dielectric properties is given in ref. [7] .

The nonlinear behavior of the STO films was determined by IMD (intermodulation distortion) measurements. Two fundamental rf signals with slightly different frequencies (here: $f_1 = 1.94$ GHz, $f_2 = 1.96$ GHz)

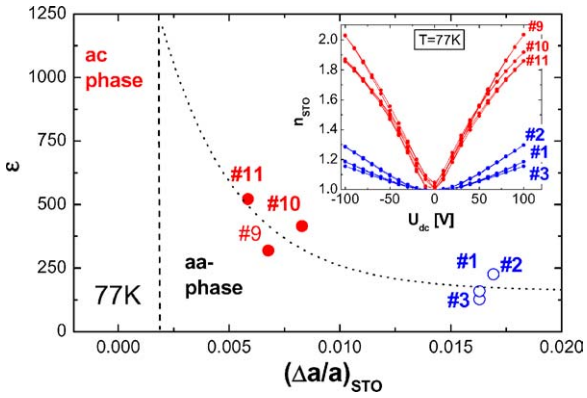

Fig. 1. Dielectric constant as function of lattice mismatch between Al_2O_3 substrate and STO film. The dotted line represent a qualitative dependence according to the Landau theory, the dashed line separates the different phases of the polarization of the STO. The inset depicts the tuneability of the different samples. The numbers refer to the sample numbers.

automatically generate higher harmonic signals and IMD signals $P_{\pm i}(i = 3, 5, 7, \ldots)$ at frequencies $f_{n,m} = nf_1 + mf_2$. The most prominent signals are the 3rd order IMD signals $P_{\pm 3}$ at $2f_1$-f_2 and $2f_2$-f_1, respectively, which are also closest to the fundamental signals (see Fig. 2).

Generally, the recorded IMD signals are relatively small. In the worst case, they exceed the noise floor at rf input-powers $P_{in} > -7$ dBm, differences of the signal levels $\Delta P = P_{in} - P_{IMD} < 40$ dB are obtained at $P_{in} > 20$ dBm. This seems to be sufficient for most applications. However, there is a clear tendency, that the IMD power level increases with increasing ε and tuneability. Thus, in case of further improvement of ε and miniaturization of the STO elements, IMD signals might become important.

However, more amazing is the power dependence of the IMD signal. All IMD signals show a similar behavior as shown in Fig. 2(b) for the 3rd order signal. At high temperature the usual linear increase with slope 3 (3rd order power dependence) is observed. At lower temperatures a second mechanism becomes visible. Starting with a linear increase with slope 2 (regime (ii)), $P_{\pm 3}$ levels off and even decreases (regime (iii)). Finally, the IMD power level increases again (regime (iv)) and joins the power dependence observed at high temperature. This unusual behavior is explained by the presence of two nonlinear properties—permittivity $\varepsilon(E)$ and conductivity $G(E)$—which is demonstrated by the two following experiments.

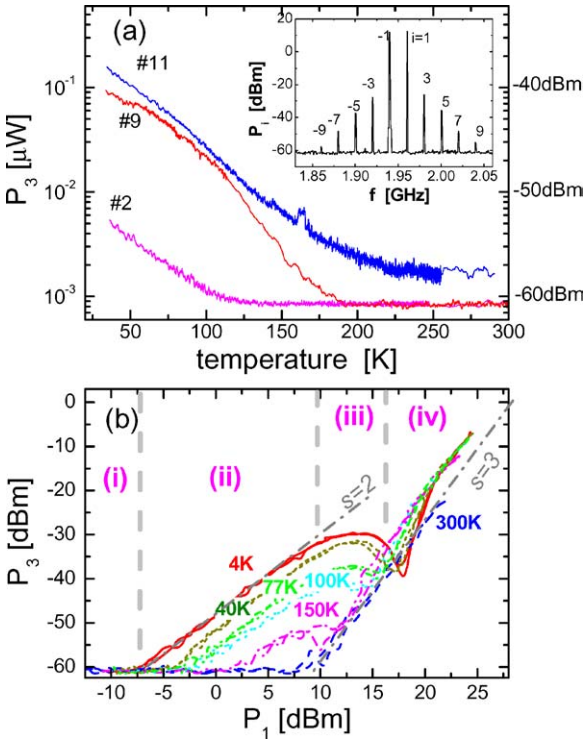

Fig. 2. (a) Temperature dependence of the 3rd order IMD signal of different STO films measured at $P_{in} = 17$ dBm (50 mW) on planar capacitors (2 μm gap width), the noise level of the experiment is ~60 dBm. The inset shows a typical spectrum of a IMD measurements with IMD signals up to the 9th order. (b) 3rd order IMD signal as function of the fundamental signal for sample #10 at different temperatures. The roman numbers mark different regimes, the dashed lines indicate different power dependences with slopes 2 and 3, respectively.

Nonlinear Relative Permittivity ε(E)

The nonlinearity of ε is a consequence of the tuneability of STO (see inset Fig. 3), i.e. a dc or rf electric field E will automatically change ε. A test of this mechanism regarding IMD generation is provided by IMD measurements with additional dc electrical field. Figure 3 shows the result of this experiment. With increasing dc field, the IMD signal is gradually suppressed in regime (ii). At $E_{dc} = 25$ V/μm (50 V) the first mechanism is removed and the measurement resembles the experiment done at 300 K (Fig. 2(b)). Thus, it seems that the first increase (and the dip) in the IMD power can be ascribed to the nonlinearity of ε.

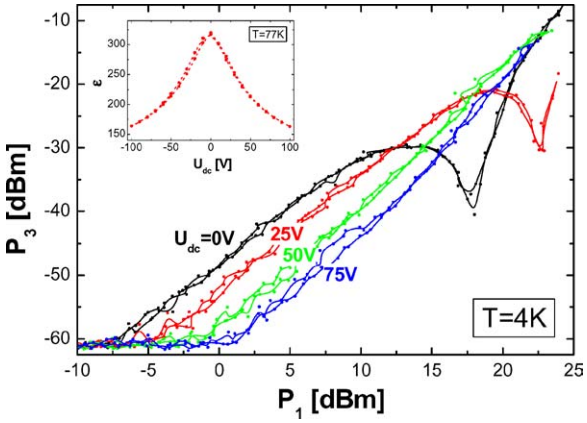

Fig. 3. 3rd order IMD signal level as function of the fundamental signal level for different dc bias voltages. The inset shows a typical dc bias dependence of ε(2 μm gap width).

Nonlinear Conductivity G(E)

In a second experiment the electric conductivity of the STO varactor is analyzed by recording the dc current due to an applied dc voltage as function of rf power level P_1. Figure 4 show a comparison of the dc conductivity and P_3 as function of P_1. There seems to be a clear correlation between the onset of conductivity and the second IMD mechanism. Similar results are obtained for other temperatures.

Finally, we compare the experiment with numerical simulation of the IMD signals. This will also reveal the origin of the unusual dip in the IMD power dependence

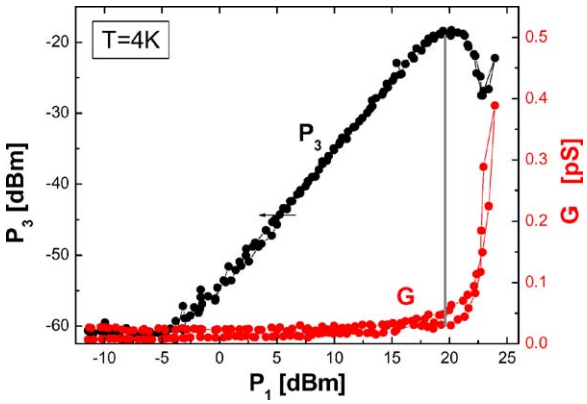

Fig. 4. Comparison of the dc conductivity and P_3 as function of rf power level P_1.

(regime iii). Usually IMD signals are theoretically described starting from a Taylor expansion of the nonlinear parameter [8]. In an attempt to parameterize the nonlinear dependence of the IMD signal of ferroelectric material, the nonlinear dependence of the electric displacement $D(E)$ would be expressed in terms of a power series [6]:

$$D(E) = \varepsilon_o \varepsilon(E) \cdot E = \sum k_i E^i = k_1 E + k_3 E^3 + k_5 E^5 \ldots \quad (1)$$

Due to symmetry reasons the odd powers of $\varepsilon(E)$ vanish. This approach leads to characteristic power dependencies of the IMD signals, i.e., $P_{\pm i}$ increases steadily and with slopes $s = i$ [8]. This is not what we observe in the experiment. Apparently there are a few shortcomings of the model: The Taylor expansion used for analytic solution of the IMD problem is usually considered up to order $n = 3$–5. This only describes the onset of the nonlinearity, whereas we are measuring up to large powers. The nonlinearity of ε and G are quite complex, e.g. $\varepsilon(E)$ seems to 'level off' at high power (see inset Fig. 3) and $G(E)$ shows a sharp onset at high power (Fig. 4). Generally, it seems to be impossible to analytically describe two nonlinear mechanisms with different onsets via this expansion up to a restricted order $n < 7$.

Thus, we developed a numerical procedure for the simulation of the IMD signal starting with a more complex field dependence of ε (see Fig. 5). The method is based on the following procedure: (i) two wave functions $E_i(t)$ of slightly different frequencies are added, (ii) the nonlinear response of the dielectric material $D(t) = \sum k_i \, [(\mathrm{E}_1^i(t) + E_2^i(t)]$ is calculated and (iii) the spectrum is derived via Fourier transformation of $D(t)$. Using an $\varepsilon(E)$ dependence that resembles the experimental curve (compare insets of Figs. 3 and 5(a)) this simulation yields intermodulation signals $P_{\pm i}$ with $i = 3, 5, 7, \ldots$ at the expected frequencies. The resolution of the simulation is restricted by the number of data points in time space. In our case (Fig. 5) data below $P_{\pm i} \approx 0.05$ are overestimated do to this limitation. Above this resolution limit, the IMD signals show a power dependence similar to the experimental data, i.e., $P_{\pm i}$ first increases with slope $s \approx 2$, followed by a leveling off, which is caused by the leveling off of the $\varepsilon(E)$-dependence. Finally the IMD signal level decreases with increasing rf input power.

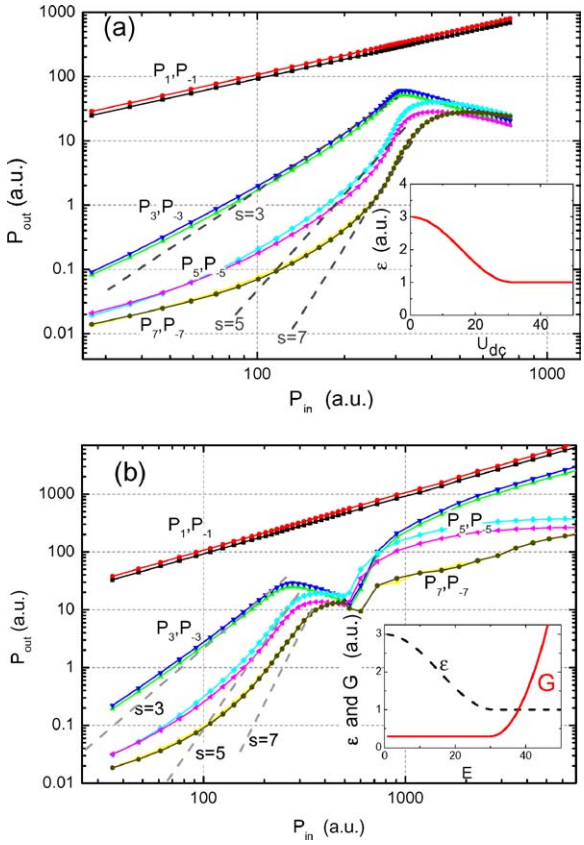

Fig. 5. Simulation of the IMD signal power P_i as function of input power. The nonlinearity of the input parameters $\varepsilon(E)$ in (a), and $\varepsilon(E)$ and $G(E)$ in (b) are sketched in the inset. All parameters are given in arbitrary units.

Adding the second mechanism (nonlinear conductivity) to the simulation by introducing a second nonlinear description of $D(t)$ with an offset (see inset Fig. 5(b)) causes a steady increase of the IMD signal level at larger power levels. The slope of this increase is defined by the exact function $D(E)$. Inserting reasonable parameters k_i for this mechanism (compare inserts Figs. 3 and 5(b)) we can simulate the complete power dependence of the IMD signals (see Fig. 5(b)).

Summary

In conclusion, ferroelectric thin films bear a large potential for the use in microwave devices due to their large tuneability and the possible integration into

complex thin film devices. However, due to size reduction the latter might lead to large rf power and, thus, potentially to nonlinear behavior. Our measurements of the resulting IMD signals of STO capacities reveal (i) that STO films possess a large power handling capability which, however, decreases with increasing ε, and (ii) that the power dependence of the IMD signals is quite unusual. Two different nonlinear mechanisms are identified, i.e. the nonlinear electric-field dependence of ε and G. A theoretical explanation in terms of a standard Taylor expansion up to order $n < 7$ of the nonlinear parameters can not explain the results. Simulation using more appropriate descriptions of ε and G up to large rf power show an excellent agreement between experimental and simulated data. The simulation procedure might be a useful tool to interpret not understood IMD results in literature [6], it might also help to unravel the mechanism responsible for the tuneability of ferroelectric thin films.

Acknowledgment

S. Bunte, P. Dymashevski, W. Hofer, E. Hollmann, R. Kutzner, N. Klein, A. Kozyrev, O. and I. Vendik.

References

1. M.B. Lee and H. Koinuma, *J. Appl. Phys.*, **81**, 2358 (1997).
2. K. Petrov and E.F. Carlsson, *J. Appl. Phys.*, **84**, 3134 (1997).
3. O.G. Vendik, E.K. Hollmann, A.B. Kozyrev, and A.M. Prudan, *J. of Supercond.*, **12**, 325 (1999).
4. K. Bouzehouane, P. Woodall, B. Marcilhac, A.N. Khodan, D. Crété, E. Jacquet, J.C. Mage, and J.P. Contour, *Appl. Phys. Lett.*, **80**, 109 (2002).
5. D. Fuchs, C.W. Schneider, R. Schneider, and H. Rietschel, *J. Appl. Phys.*, **85**, 7362 (1999).
6. N.A. Pertsev, A.G. Zembilgotov, and A.K. Tagantsev, *Physical Review Letters*, **80**(9), 1988 (1998).
7. R. Ott and R. Wördenweber, in preparation.
8. M. Hein, *High-Temperature-Superconductor Thin Films at Microwave Frequencies* (Spinger-Verlag, 1999), ISSN 0081-3869, ISBN 3-540-65646-4.